Journal of Catalysis 285 (2012) 187–195

Contents lists available at SciVerse ScienceDirect

Journal of Catalysis

journal homepage: www.elsevier.com/locate/jcat

Ethylene conversion to ethylidyne on Pd(1 1 1) and Pt(1 1 1): A first-principles-based kinetic Monte Carlo study

Hristiyan A. Aleksandrov [a,b], Lyudmila V. Moskaleva [a,c], Zhi-Jian Zhao [a], Duygu Basaran [a], Zhao-Xu Chen [a,d], Donghai Mei [e,*], Notker Rösch [a,*]

[a] Department Chemie and Catalysis Research Center, Technische Universität München, 85747 Garching, Germany
[b] Faculty of Chemistry, University of Sofia, 1126 Sofia, Bulgaria
[c] Institut für Angewandte and Physikalische Chemie, Universität Bremen, 28359 Bremen, Germany
[d] Institute of Theoretical and Computational Chemistry, Key Laboratory of Mesoscopic Chemistry of MOE, School of Chemistry and Chemical Engineering, Nanjing University, Nanjing 210093, PR China
[e] Institute for Interfacial Catalysis, Pacific Northwest National Laboratory, Richland, WA 99352, USA

ARTICLE INFO

Article history:
Received 2 June 2011
Revised 9 September 2011
Accepted 24 September 2011
Available online 25 November 2011

Keywords:
Ethylene conversion
Ethylidyne
Vinylidene
First-principles-based kinetic Monte Carlo simulations
Pd(1 1 1)
Pt(1 1 1)
Metal catalysts
DFT calculations

ABSTRACT

We present kinetic Monte Carlo simulations of ethylene conversion to ethylidyne on Pd(1 1 1) and Pt(1 1 1) surfaces, on the basis of reaction enthalpies and barriers obtained from periodic density functional calculations. We considered three possible mechanisms encompassing four different intermediates, ethyl, vinyl, ethylidene, and vinylidene. Our simulations predict that the most plausible pathway on both surfaces is ethylene → vinyl → vinylidene → ethylidyne. In contrast to earlier suggestions that the dehydrogenation to vinyl is rate-limiting on Pt(1 1 1), we found the hydrogenation of vinylidene to ethylidyne to be crucial on this surface. On Pd(1 1 1), the initial dehydrogenation of ethylene is rate-limiting. Hence, vinylidene species accumulate on Pt(1 1 1), while all intermediates on Pd(1 1 1) convert rapidly to ethylidyne without accumulation. The simulated apparent activation energies for the formation of ethylidyne on Pd(1 1 1), 94 kJ mol^{-1}, and on Pt(1 1 1), 65 kJ mol^{-1}, agree well with experimental results.

1. Introduction

One of the main goals of theoretical chemistry is to understand the complex mechanisms of chemical reactions. Olefins constitute a very important class of organic compounds with wide application in petrochemistry, organic, and polymer chemistry. As the simplest alkene, ethylene provides a prototype system for understanding various transformations of alkenes on metal surfaces. Transition metals are frequently used to catalyze alkene transformations; therefore, a deeper understanding of the interaction between ethylene and transition metals is of great interest to catalysis.

Two types of adsorption modes are known for ethylene adsorbed on transition metal surfaces [1–10], the π-adsorbed mode, which is stable at very low temperatures, e.g., below 52 K on Pt(1 1 1), and the di-σ adsorbed mode which dominates on the surface up to ~250 K. When ethylene is further heated on Pd(1 1 1) [9–14] and Pt(1 1 1) [1,6,7,15,16], a stable phase of ethylidyne species starts to form on the surface. An analogous decomposition of ethylene to ethylidyne has also been observed on other transition metal surfaces such as Rh(1 1 1) [17], Ir(1 1 1) [18], and Ru(0 0 0 1) [19]. Stable and hardly removable ethylidyne deposits cover the metal surface during ethylene hydrogenation over Pt(1 1 1) or Pd(1 1 1). They can be decomposed only at temperatures above 400 K [12,20–23].

Thus, ethylene conversion to ethylidyne can be viewed as fundamental and important for understanding the chemistry of ethylene on transition metal surfaces in general. Yet, the complex conversion mechanism on various transition metal surfaces is under discussion. Therefore, recent theoretical studies considered various possible pathways of this process on the surfaces Pd(1 1 1) [24–28], Pt(1 1 1) [29,30], and Rh(1 1 1) [31]. For an overview of pertinent experimental work on Pt(1 1 1), see e.g. Ref. [32].

The mechanism of this conversion may include at least four intermediates: vinyl CH_2CH, vinylidene CH_2C, ethylidene CH_3CH, and ethyl CH_3CH_2. On the basis of several experimental kinetic and spectroscopic studies of ethylene transformations on Pt(1 1 1), Zaera and French [32] suggested a two-step mechanism, via an isomerization to ethylidene (1,2-H shift reaction), followed by a

* Corresponding authors.
E-mail address: roesch@mytum.de (N. Rösch).

0021-9517/$ - see front matter © 2011 Elsevier Inc. All rights reserved.
doi:10.1016/j.jcat.2011.09.035

dehydrogenation to ethylidyne. However, theoretical studies by other groups [28,33] as well as our own recent calculations [24,29] showed that the direct 1,2-H shift reaction from ethylene to ethylidene requires a very high activation energy on both Pd and Pt, above 200 kJ mol^{-1}, suggesting that the mechanism is more complex. Recently, we examined three pathways with a computational method based on density functional theory (DFT; see Fig. 1): (i) Mechanism 1 via vinyl and ethylidene (M1: R*a* → R*b* → R*f* → R*e*), (ii) Mechanism 2 via vinyl and vinylidene (M2: R*a* → R*b* → R*g* → R*h*), and (iii) Mechanism 3 via ethyl and ethylidene (M3: R*a* → R*i* → R*j* → R*e*). We compared the reaction energy landscapes at three surface coverages, 1/3, 1/4, and 1/9 of a monolayer [34] on Pd(1 1 1) [24,27] and Pt(1 1 1) [29], applying a DFT-based method to periodic slab models. We calculated barriers of 1,2-H shift reactions typically above 160 kJ mol^{-1}, i.e., significantly higher than the barriers determined for hydrogenation–dehydrogenation steps. Hence, pathways that include 1,2-H shift reactions were ruled out from the discussion.

Our results on Pd(1 1 1) showed that mechanisms M1 and M2 appear to be equally plausible, where in both cases the first and common step, namely, the dehydrogenation of ethylene to vinyl (reaction R*b*, Fig. 1) was concluded to be rate-limiting [24,27]. At 1/3 coverage, the barrier for hydrogenation of vinyl to ethylidene (R*f*) is 10 kJ mol^{-1} lower than the barrier for vinyl dehydrogenation to vinylidene (R*g*), while at 1/9 coverage, the situation is opposite [27]. Similar to our findings on Pd(1 1 1), mechanisms M1 and M2 likely also compete over Pt(1 1 1), in the absence of coadsorbed hydrogen [29]. However, comparison of the potential energy landscapes on both metal surfaces also reveals characteristic differences. On the basis of calculated barriers, we were able to identify the first step (R*b*) as the rate-limiting on Pd(1 1 1), whereas this was not fully clear in the case of Pt(1 1 1), especially at 1/9 coverage where several reaction steps have similar barriers, ~75 kJ mol^{-1} [29].

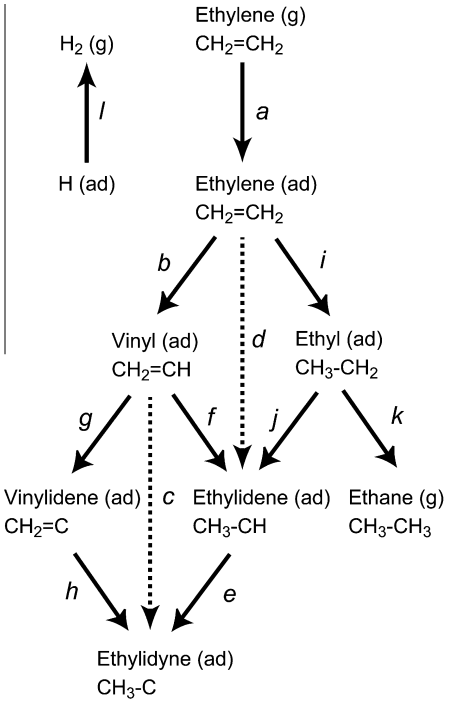

Fig. 1. Reaction pathways of ethylene conversion to ethylidyne over Pt group metals. Arrows pointing to the left and right indicate dehydrogenation and hydrogenation steps, respectively. Arrows pointing downward and upward represent adsorption and desorption, respectively. Arrows rendered as dotted lines indicate 1,2 H shift reactions. Letters *x* close to the arrows designate elementary reaction steps that are referred as R*x* in the text. The following mechanisms are being discussed: (i) Mechanism 1 via vinyl and ethylidene (M1: R*a* → R*b* → R*f* → R*e*), (ii) Mechanism 2 via vinyl and vinylidene (M2: R*a* → R*b* → R*g* → R*h*), and (iii) Mechanism 3 via ethyl and ethylidene (M3: R*a* → R*i* → R*j* → R*e*).

In addition to mechanisms M1 and M2, a third mechanism, M3, via ethyl and ethylidene, may also play a role on both metal surfaces when the atomic H coverage is high enough. Analysis of the barriers involved in M3 shows that they are lower or comparable to the highest barriers of M1 and M2. Another DFT study reported similar results for ethylene conversion on Pd(1 1 1) and Pd(2 1 1) [28]. Here, however, one should keep in mind that ethyl, which is formed during reaction R*i* via hydrogenation of ethylene, can easily be hydrogenated to ethane (R*k*) [27,29,35–37]. Specifically, at 1/9 coverage, the barriers for reaction R*k* were calculated quite low, 51 kJ mol^{-1} on Pd(1 1 1) [27] and 77 kJ mol^{-1} on Pt(1 1 1) [29].

Although our DFT calculations suggested plausible mechanisms of ethylene conversion to ethylidyne, we were unable to determine unequivocally which particular pathway should be dominating at given experimental conditions. Further clarification of the mechanistic picture can be achieved by kinetic modeling with macroscopic rate equations or, preferably, by kinetic Monte Carlo (kMC) simulations. The latter allow one to track explicitly the behavior of all surface species as function of time and processing conditions [38–43]. We, therefore, turned to kMC simulations in the present work, employing a first-principles kinetic database, constructed from our DFT results, in combination with a parameterized semi-empirical model for lateral interactions to account for effects of the local environment on the kinetics [44–50]. This combined DFT/kMC approach maintains important atomic features of a catalytic metal surface and can therefore be used to probe how various competing reaction steps may affect the activity and selectivity of the catalyst. Previously, this approach was successfully used, for instance, to examine the decomposition of acetic acid on Pd(1 1 1) [46], as well as the hydrogenation of ethylene on Pd(1 1 1) [45] and Pd/Au(1 1 1) [47,48] and of acetylene on Pd(1 1 1) [50], and Pd/Ag(1 1 1) [42].

2. Method

We employed the *variable time step* kinetic Monte Carlo algorithm as previously described [45–50]. The intrinsic kinetic database used in our simulations (Tables 1 and 2) is based on our recent periodic DFT calculations [26,27,29]. These DFT calculations had been carried out with the plane-wave based Vienna ab initio simulation package VASP [51,52], employing the exchange–correlation functional PW91, a generalized-gradient approximation (GGA) [53]. Detailed information about our model strategy is available in Refs. [26,27,29].

Table 1
Atomization energies (E_{at}, kJ mol^{-1}) and binding energies (BE, kJ mol^{-1}) of all the considered surface species on Pd(1 1 1) and Pt(1 1 1).

Species	E_{at}	BE on Pd(1 1 1)			BE on Pt(1 1 1)		
		Atop	Bridge	Hollow	Atop	Bridge	Hollow
Hydrogen (H)	–	226	263	276	268	263	267
Hydrogen (H_2)	440	20	20	–	20	20	–
Ethylene	2414	78	90	–	84	121	–
Ethylidyne	1720	–	–	553	–	–	592
Vinyl	1935	–	–	273	–	–	324
Vinylidene	1569	–	–	394	–	–	441
Ethylidene	2115	–	357	–	–	389	0
Ethyl	2581	164	–	–	195	–	–
Ethane	3023	18	18	–	18	18	–

Table 2
Activation barriers (kJ mol^{-1}) of the forward (E^{for}) and backward (E^{back}) reaction steps considered on Pd(1 1 1) and Pt(1 1 1).

N[a]	Reaction	Barriers on Pd(1 1 1)		Barriers on Pt(1 1 1)	
		E^{for}	E^{back}	E^{for}	E^{back}
b	$CH_2CH_2^* \rightarrow CH_2CH^* + H^*$	100	73	75	61
i	$CH_2CH_2^* + H^* \rightarrow CH_3CH_2^*$	85	57	88	65
k	$CH_3CH_2^* + H^* \rightarrow CH_3CH_3$	51	79	77	64
g	$CH_2CH^* \rightarrow CH_2C^* + H^*$	57	78	53	69
h	$CH_2C^* + H^* \rightarrow CH_3C^*$	78	120	80	116
f	$CH_2CH^* + H^* \rightarrow CH_3CH^*$	77	72	79	61
−e	$CH_3C^* + H^* \rightarrow CH_3CH^*$	84	25	89	19
−j	$CH_3CH^* + H^* \rightarrow CH_3CH_2^*$	80	81	67	74
l	$H^* + H^* \rightarrow H_2$	83	1	83	6

[a] Notation according to Fig. 1.

The data for the binding energies (Table 1) and intrinsic barriers (Table 2) were taken as calculated for the largest unit cell modeled, (3 × 3), as the adsorbate–adsorbate interactions are accounted for separately in the kMC simulations [45]. In the kMC models, we simulated the conversion of ethylene on the (1 1 1) surface of Pt or Pd, represented by a periodic 16 × 16 lattice of metal atoms containing 1024 different surface sites (atop, bridge, and threefold hollow sites). Each adsorbate was allowed to occupy one or two sites of a certain type as determined by DFT calculations [26,27,29]. Test calculations using a 32 × 32 lattice of metal atoms yielded reaction rates and surface coverages close to those obtained for the (standard) 16 × 16 lattice.

The zero-point-energy corrections were not taken into account. Such corrections are expected to be on the order of 10–15 kJ mol^{-1} [54], as confirmed here by a check for the rate-limiting step, ethylene dehydrogenation to vinyl on Pd(1 1 1) (see Section 3.1) and are thus within the accuracy of our DFT approach.

Diffusion of the species on the surface can be explicitly simulated, neglected or treated as quasi-equilibrated. We have chosen to treat the diffusion of surface intermediates herein as being quasi-equilibrated. According to earlier studies on the hydrogenation of ethylene [47,48], diffusion of intermediates does not significantly affect the results.

During the conversion of ethylene to ethylidyne on Pd(1 1 1) and Pt(1 1 1), the metal surface becomes less "active" toward the end of a simulation because the product species, ethylidyne, is adsorbed so strongly on the transition metal surfaces that its desorption at the temperatures investigated is not possible. Remaining on the surface, it reduces the active sites available for ethylene conversion and, in this way, it "poisons" the surface. Therefore, the reaction rates of most of the elementary steps increase at the beginning of the simulations, but they start to drop as soon as ethylidyne is formed intensively. The rates shown in Figs. 2 and 3 are determined after simulating processes of 1 s where the metal surfaces are still active even at high temperatures. The qualitative relationships between the rates of the elementary reactions do not change during the whole of a simulation; hence, we shall limit the discussion to the representative snapshots of Figs. 2 and 3. For some less important reaction steps where the rates are still essentially zero at 1 s, we will give the maximum values reached during the simulation, only to illustrate that these maximum values are still significantly lower than the rates of other important reaction steps.

3. Results and discussion

3.1. Ethylene conversion to ethylidyne on Pd(1 1 1)

We started the simulations with a clean metal surface and the partial pressure of ethylene at 1 torr. We carried out simulations at various temperatures. The reaction of ethylene to ethylidyne started on Pd(1 1 1) at 330 K, while ethylidyne starts to decompose above 400 K, the highest temperature we explored [12,20–23]. The reaction rates increase with temperature, as shown in Fig. 2 for Pd(1 1 1). The only exception is the rate of ethylene adsorption that decreases when the temperature increases, due to a $\sim T^{-0.5}$ dependence in the pre-exponential factor [44]. We also examined how the reaction rates depend on the partial pressure of ethylene, but we did not find significant changes in the reaction rates when the partial pressure of ethylene was varied in the range 1–100 torr. Hence, we will base our discussion on the results obtained for $P(C_2H_4)$ = 1 torr.

Next, we will successively address all surface species considered, namely, ethylene, vinyl, vinylidene, ethyl, ethylidene, ethylidyne, and hydrogen, discussing in each case the competition between possible reaction events.

3.1.1. Ethylene

At the investigated temperatures, T > 200 K, the di-σ adsorption mode of ethylene is more stable on both surfaces than π-adsorbed ethylene. Therefore, we considered only di-σ adsorbed ethylene as the reactant. π-adsorbed ethylene is stable at very low temperatures (below 50 K) or at hydrogen pre-covered surfaces. Both situations are not relevant to the present study. When an ethylene molecule adsorbs on the surface, three types of events can occur (Fig. 1): (i) desorption from the metal surface (R–*a*, reverse reaction of R*a*), (ii) dehydrogenation to vinyl (R*b*), or (iii), if hydrogen is available nearby, hydrogenation to ethyl (R*i*). The desorption and hydrogenation processes have similar rates; they are about an order of magnitude faster than dehydrogenation (Fig. 2). However, as in our simulations, the external partial pressure of ethylene was chosen at 1 torr, the adsorption rate of ethylene is about one order of magnitude larger than the desorption rate, especially at the beginning of the simulations. This provides enough ethylene molecules on the surface. Reaction *Ri* is about six times faster than R*b*, as the barrier of ethylene hydrogenation, 85 kJ mol^{-1}, is lower by 15 kJ mol^{-1}, than that for its dehydrogenation, 100 kJ mol^{-1} (Table 2). However, the latter reaction step is practically irreversible, while the forward reaction to form ethyl (R*i*) and the corresponding backward reaction have essentially the same rates. Facile desorption of ethylene from Pd(1 1 1) and the reversibility of ethylene hydrogenation are two features that render Pd an excellent catalyst for the selective hydrogenation of acetylene in mixtures of acetylene and ethylene [55].

3.1.2. Vinyl

Vinyl species may undergo three types of events on Pd(1 1 1), Fig. 1: hydrogenation (i) to ethylene (R–*b*) or (ii) to ethylidene (R*f*), and (iii) dehydrogenation to vinylidene (R*g*). The latter event is faster by more than five orders of magnitude than the other two (Fig. 2). This is not surprising because the barrier for reaction

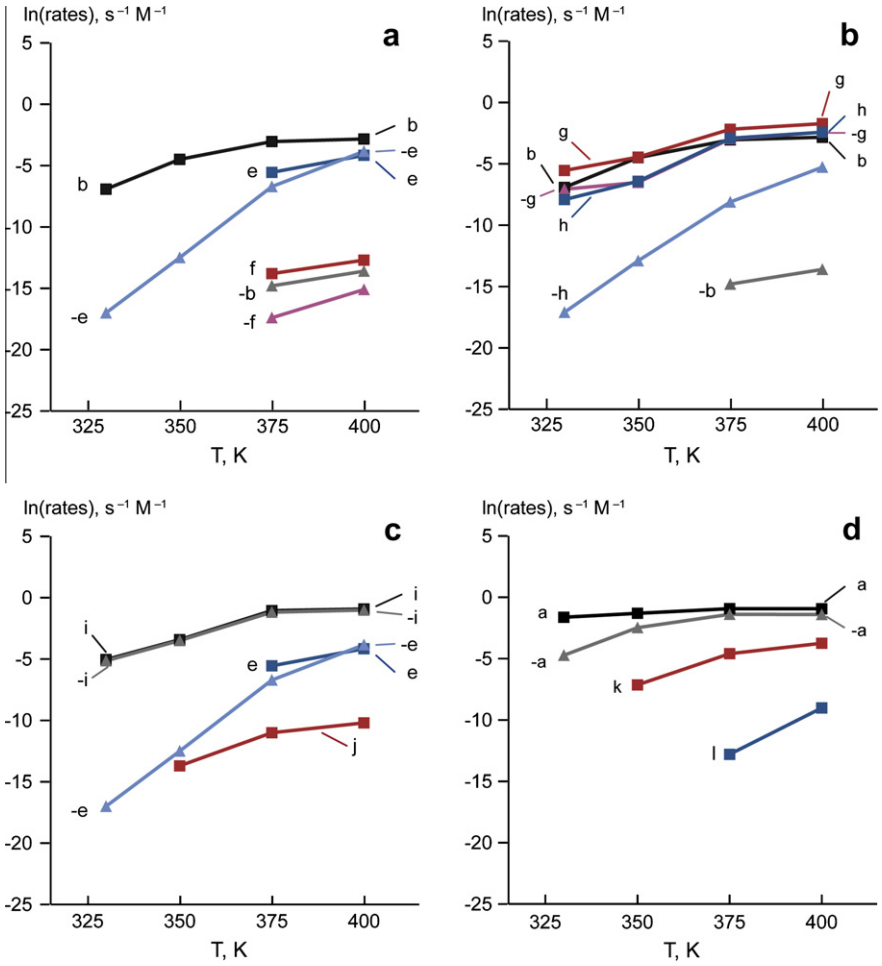

Fig. 2. Dependence on temperature of the reaction rates at $t = 1$ s of the various reaction steps during ethylene conversion to ethylidyne on Pd(1 1 1) according to the mechanisms (a) M1, (b) M2, and (c) M3. Also shown (d) are additional reaction steps related to the adsorption or desorption of ethylene, ethane, and hydrogen for elementary reactions forward and backward (–) (see Fig. 1 for a-l). Reaction rates are essentially zero in cases where data points are missing.

Rg, 57 kJ mol^{-1}, is 16–20 kJ mol^{-1} lower than the two hydrogenation barriers (Table 2). In addition, hydrogenation reactions are limited by the supply of H atoms on the surface in the vicinity of the vinyl species.

3.1.3. Vinylidene

Vinylidene species can convert to ethylidyne species (R*h*) or back to vinyl (R–*g*). As both reaction steps have essentially the same barriers, 78 kJ mol^{-1} (Table 2), they also have very similar rates (Fig. 2b). In fact, reaction R–*g* is slightly faster than R*h*, while the formation of ethylidyne (R*h*) is irreversible (Fig. 2). Hence, vinylidene species can convert to ethylidyne.

3.1.4. Ethyl

Ethyl species can be dehydrogenated (i) to ethylidene (R*j*) or (ii) to ethylene (R–*i*), or (iii) they can be hydrogenated to ethane (R*k*). Reaction R–*i* is the fastest but, as mentioned above, it is at equilibrium. Reaction R–*i* is one to two orders of magnitude faster than R*k* (Fig. 2), despite the fact that both reaction steps exhibit almost equal barrier heights, 57 and 51 kJ mol^{-1}, respectively (Table 2). However, surface hydrogen is required for the hydrogenation and the conversion to ethane is completely irreversible. The transformation of ethyl to ethylidene (R*j*) is significantly slower than the other two reactions (Fig. 2), as a consequence of the significantly higher barrier, 81 kJ mol^{-1} (Table 2).

3.1.5. Ethylidene

Ethylidene species on the surface can undergo three types of reactions: (i) hydrogenation to ethyl (R–*j*), or dehydrogenation to (ii) ethylidyne (R*e*) or (iii) vinyl (R–*f*). At low temperatures, 330 K and 350 K, none of these reactions occur as ethylidene also forms in a slow process, whereas, at the higher temperature 400 K, R*e* dominates. Because of the remarkably low barrier of this reaction step, 25 kJ mol^{-1} (Table 2), it is more than five orders of magnitude faster than the other two transformations (Fig. 2).

3.1.6. Ethylidyne

Ethylidyne species can be dehydrogenated to vinylidene (R–*h*) or hydrogenated to ethylidene (R–*e*). The barrier for the former, 120 kJ mol^{-1}, is 36 kJ mol^{-1} higher than the barrier for the latter, 84 kJ mol^{-1} (Table 2). Thus, R–*e* is about one order of magnitude faster than R–*h* (Fig. 2).

3.1.7. Hydrogen

For each molecule of ethylene converted to ethylidyne, a hydrogen atom is produced on the Pd(1 1 1) surface. Hydrogen can either recombine and desorb from the surface as H_2 or it can react with ethylene. In the latter case, after two subsequent hydrogenation steps, ethane can be produced. Our results show that the rate of ethane formation on Pd(1 1 1) is 2–4 orders of magnitude higher than the rate of forming H_2 (Fig. 2d), again in consequence of relative barrier heights. The barrier of ethyl hydrogenation (R*k*),

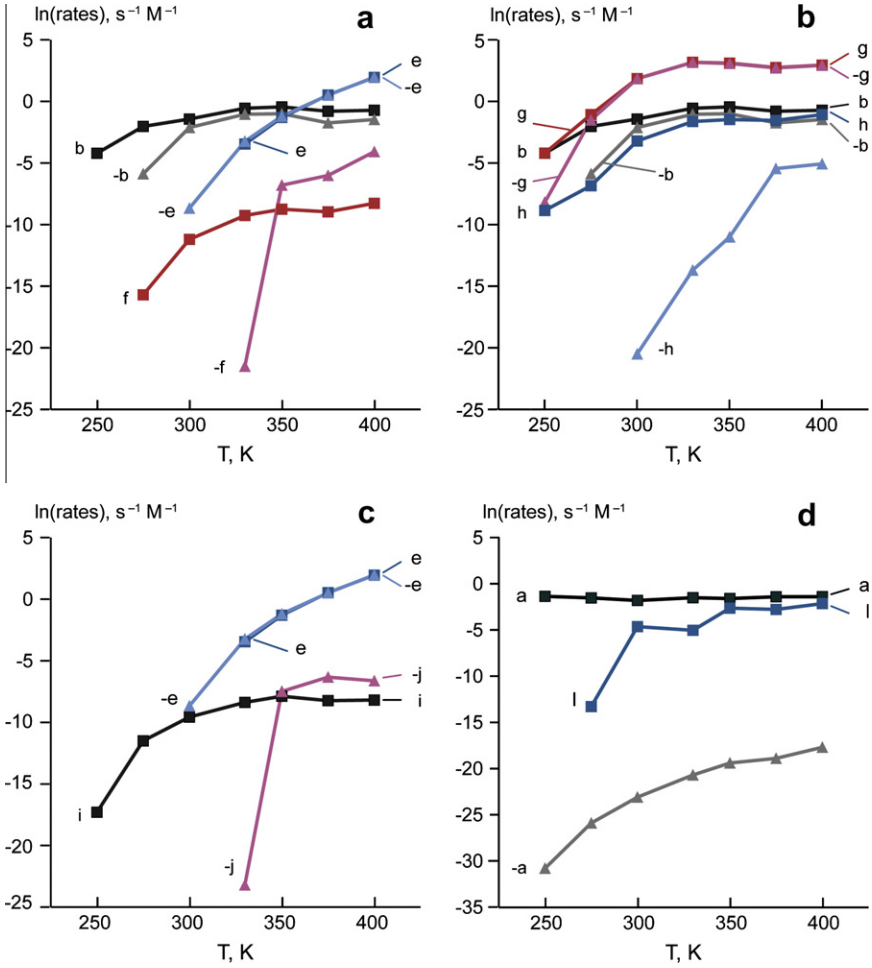

Fig. 3. Dependence on temperature of the reaction rates at $t = 1$ s of the various reaction steps during ethylene conversion to ethylidyne on Pt(1 1 1) according to the mechanisms (a) M1, (b) M2, and (c) M3. Also shown (d) are additional reaction steps related to the adsorption or desorption of ethylene, ethane, and hydrogen for elementary reactions forward and backward (–) (see Fig. 1 for a-l). As ethylidyne formation starts at 250 K, the rates at 230 K are not shown. Reaction rates are essentially zero in cases where data points are missing.

51 kJ mol^{-1}, is notably lower than the barrier of H recombination (R*l*), 83 kJ mol^{-1} (Table 2). Temperature programmed desorption (TPD) studies [12,56] of ethylene deposited on clean Pd(1 1 1) also found that mainly ethane desorbs at ~310 K, while a very small amount of H_2 is detected below 400 K (at 350 K). These experiments found H_2 to be mainly produced at ~425 K, which corresponds to the thermal decomposition of ethylidyne, a process not considered in the present kMC simulations. In a recent DFT study [54], we showed that the most plausible pathway of ethylidyne decomposition, $CCH_3 \rightarrow CCH_2 \rightarrow CCH$, requires overcoming a barrier as high as 138 kJ mol^{-1}. In other words, such a process is not expected to occur at temperatures below 400 K.

3.1.8. Discussion of mechanisms

Next, we compare the three mechanisms, M1 to M3, by identifying the rate-limiting step [57] in each of them and by examining which one is the fastest mechanism. That should be the dominating mechanism at a given *T*.

Our simulations of ethylene conversion to ethylidyne on Pd(1 1 1) show that the rate-limiting step of M1 is the hydrogenation of vinyl to ethylidene (R*f*, Fig. 2a), whereas in M2, the slowest step R*b* (ethylene dehydrogenation to vinyl) determines the overall conversion rate (Fig. 2b). In M3, the slowest step, with an almost vanishing rate, is ethyl dehydrogenation to ethylidene (R*j*). Among these rate-limiting steps, R*b* is the fastest. Hence, at the reaction conditions explored on Pd(1 1 1), M2 clearly is the most plausible mechanism for ethylene conversion to ethylidyne. This result may seem a bit surprising because, considering only reaction barriers, one would expect R*b* with a barrier of 100 kJ mol^{-1} to be the slowest step in both M1 and M2. The barriers of reactions R*f*, R*h*, and R*i* are all lower: 77 kJ mol^{-1}, 78 kJ mol^{-1}, 80 kJ mol^{-1}, respectively. The reason for this seeming contradiction is the fact that hydrogenation steps require a substantial amount of hydrogen on the surface, which apparently is not available at the simulated initial reaction conditions, where only ethylene, but no H_2 are supplied in the gas phase. Moreover, the atomic H produced on the surface in the course of the conversion can desorb as H_2 or C_2H_6.

To probe the sensitivity of our results to the barrier heights of those reaction steps with the highest barriers, we reduced the barriers for forward and backward reaction of ethylene dehydrogenation to vinyl by 10–15 kJ mol^{-1}. This did not alter our conclusions regarding the rate-limiting steps.

This analysis nicely illustrates one of the major advantages of the kMC method, namely its ability to provide more direct and conclusive information about the process at pertinent reaction conditions than a simple analysis of barriers and reaction energies.

3.2. Ethylene conversion to ethylidyne on Pt(1 1 1)

Using the same initial conditions as for Pd(1 1 1), we carried out simulations of the conversion of ethylene to ethylidyne on Pt(1 1 1) at 1 torr partial pressure of ethylene. Fig. 3 shows the reaction rates

of the various pathways on Pt(1 1 1) as a function of temperature. On Pt(1 1 1), ethylene dehydrogenation starts at a significantly lower temperature, at 230 K, than on Pd(1 1 1) (from 330 K). Therefore, we examined a wider range of temperatures, 230–400 K, compared to Pd(1 1 1). These findings agree with experiments [58] where ethylene conversion to ethylidyne was found to start at a lower temperature on Pt(1 1 1), above 270 K [6], than on Pd(1 1 1), from 300 K [10].

3.2.1. Ethylene

When ethylene adsorbs on Pt(1 1 1), its dehydrogenation to vinyl (R*b*) is the fastest reaction step. It is three to six orders of magnitude faster than ethylene hydrogenation to ethyl (R*i*). The barrier of R*i*, 88 kJ mol^{-1}, is 13 kJ mol^{-1} higher than that of reaction R*b*, 75 kJ mol^{-1}. This result also allows us to rationalize why the hydrogen generated during the conversion of ethylene to ethylidyne does not suffice for producing a substantial amount of ethyl on the surface. Experiments detected ethyl species when ethylene is hydrogenated on Pt catalyst [59,60]; however, when the reactant mixture contains only pure ethylene (no H_2), such species are not detected, in line with our kMC results. In contrast to the situation on Pd(1 1 1), the third possible reaction step, ethylene desorption, is significantly slower on Pt(1 1 1) than the two reaction steps just mentioned, due to the very high adsorption energy of ethylene on Pt(1 1 1), 121 kJ mol^{-1} (Table 1). Ethylene desorption was calculated 7–13 orders of magnitude slower than ethylene adsorption: ethylene molecules "stick" very well on Pt(1 1 1). This finding is at variance with the experimental studies which found ethylene to start desorbing from Pt(1 1 1) at ~220 K [1] with a peak at $T \approx 285$ K [61]. However, temperature programmed desorption (TPD) measurements suggested an adsorption energy of di-σ ethylene on Pt(1 1 1), 71 kJ mol^{-1} [62,63], significantly lower than our GGA results. As previously remarked [29], this discrepancy between theory and experiment is not too surprising because the GGA functional PW91, used in our DF calculations, is known to overestimate systematically chemisorption energies by up to 50 kJ mol^{-1} [64]. Relative energies are expected to be more accurate. We checked the sensitivity of our simulations to the binding energy of ethylene, using a value lower by 30 kJ mol^{-1}. In consequence, the rate of ethylene desorption increased significantly and was only about one order of magnitude slower than the rate of ethylene adsorption at 330 K. However, the overall conclusions about the preferred mechanism of ethylene conversion and the rate-limiting steps were not altered in this "computer experiment".

Comparing Pt(1 1 1) and Pd(1 1 1), we note that Wang et al. [58] observed ethylene desorption from Pd(1 1 1) at 100–350 K without significant decomposition, while Berlowitz et al. [65] calculated the fraction of ethylene decomposing at about 35% for saturation coverage on Pt(1 1 1), compared to only 2% on Pd(1 1 1). These results manifest a significantly easier desorption of ethylene from Pd(1 1 1) than from Pt(1 1 1), in combination with significantly easier ethylene dehydrogenation on Pt(1 1 1) than on Pd(1 1 1). Both experimental findings are in line with our computational results.

3.2.2. Vinyl

Similar to the observations on Pd(1 1 1), vinyl species on Pt(1 1 1) can be easily dehydrogenated to vinylidene (Rg). This conclusion agrees with experiments of Zaera and Bernstein [15] who found vinyl to convert to vinylidene on Pt(1 1 1) at temperatures as low as ~140 K. To check these results, we also carried out simulations starting with vinyl species adsorbed initially on Pt(1 1 1) and Pd(1 1 1) [66]. These simulations confirmed that the conversion of vinyl species to vinylidene starts at 140 K on both surfaces. Step Rg is about two orders of magnitude faster than vinyl hydrogenation to ethylene (R–*b*) (or about six orders of magnitude faster than hydrogenation of vinyl to ethylidene, R*f*) (Fig. 3). These results are in line with the lower barrier of Rg, 53 kJ mol^{-1}, compared to the barriers of steps R–*b* and R*f*, 61 kJ mol^{-1} and 79 kJ mol^{-1} (Table 2), respectively, and with the dependence of the hydrogenation reactions on the presence of hydrogen at the surface.

3.2.3. Vinylidene

The barrier for the hydrogenation of vinylidene to vinyl (R–*g*), 69 kJ mol^{-1}, is 11 kJ mol^{-1} lower than the barrier for the hydrogenation to ethylidyne (R*h*), 80 kJ mol^{-1} (Table 2). Hence, R–*g* is about two orders of magnitude faster than R*h* (Fig. 3), while on Pd(1 1 1) both reaction steps were calculated to have similar rates (Fig. 2). Nevertheless, as on Pd(1 1 1), R–*g* is at equilibrium whereas R*h* is essentially irreversible on Pt(1 1 1). This enables ethylidyne formation via M2 on Pt(1 1 1).

The discussed differences between the surfaces Pt(1 1 1) and Pd(1 1 1) are corroborated by experiments [67] where on Pd(1 1 1) vinyl was observed to convert rapidly to ethylidyne at low temperatures (160 K), whereas on Pt(1 1 1) this reaction occurs only around 300 K [15]. To further examine the unequal behavior of the intermediates vinyl and vinylidene on the two metal surfaces, we used the simulations mentioned above [66] starting with vinyl species on the metal surface. In qualitative agreement with the experiments just mentioned, [15,67] these simulations revealed that vinyl converts to ethylidyne on Pt(1 1 1) at 250 K (at the same temperature as required for ethylene conversion). In contrast, on Pd(1 1 1) vinyl was calculated to convert to ethylidyne at 230 K, which is 100 K lower than the temperature of ethylene conversion to ethylidyne on Pd(1 1 1). The latter result is consistent with the first step (R*b*) being rate-controlling on Pd(1 1 1).

3.2.4. Ethyl

During the first several seconds of the simulation, the three reaction steps in which ethyl species are involved (R–*i*, R*j*, and R*k*) have essentially zero rates (not shown in Fig. 3). Even when their rates reach maximum values, they are significantly lower than the rates of reaction steps that involve vinyl or vinylidene. Similar to the situation on Pd(1 1 1), the fastest reaction among those three is again dehydrogenation of ethyl to ethylene R–*i*, not shown in Fig. 3). It has a lower barrier, 65 kJ mol^{-1}, than the dehydrogenation to ethylidene (R*j*), 74 kJ mol^{-1}, and the hydrogenation to ethane (R*k*), 77 kJ mol^{-1} (Table 1). Therefore, it is one to three orders of magnitude faster than the latter reactions (not shown in Fig. 3).

3.2.5. Ethylidene

The rates of the reaction steps involving ethylidene species are essentially zero for temperatures below 300 K. At higher temperatures, ethylidene dehydrogenation to ethylidyne (R*e*) on Pt(1 1 1), having a remarkably low barrier of only 19 kJ mol^{-1} (Table 2), is faster by 3–8 orders of magnitude than the other two reactions (Fig. 3), which have significantly higher barriers, namely, ethylidene dehydrogenation to vinyl (R–*f*), 61 kJ mol^{-1}, and ethylidene hydrogenation to ethyl (R–*j*), 67 kJ mol^{-1}.

3.2.6. Ethylidyne

The hydrogenation of ethylidyne to ethylidene (R–*e*) is three to five orders of magnitude faster than its dehydrogenation to vinylidene (R–*h*) (Fig. 3), due to the lower barrier of the former reaction, 89 kJ mol^{-1}, compared to the latter, 116 kJ mol^{-1} (Table 2). A similar situation was already discussed for Pd(1 1 1).

3.2.7. Hydrogen

Recall that surface hydrogen is removed from Pd(1 1 1) as ethane (R*i* and R*k*) rather than as H_2 (R*l*). The situation on Pt(1 1 1) is opposite due to the relatively high barriers for ethylene and ethyl hydrogenation, 88 kJ mol^{-1} and 77 kJ mol^{-1}, respectively (Table 2),

and the lower barrier of β–H elimination from ethyl (R–*i*), 65 kJ mol^{-1} (see Fig. 5c of Ref. [29]). Hence, surface hydrogen can recombine to form H_2 and desorb from Pt(1 1 1) significantly faster than ethane can be formed because the barrier for H recombination is 83 kJ mol^{-1} (Table 2). Experiments also found that from Pt(1 1 1) significantly more H_2 desorbs than ethane [1,16,65].

3.2.8. Discussion of mechanisms

Just as for Pd(1 1 1), our kMC results on Pt(1 1 1) thus showed that the rate-liming steps of the mechanisms M1 and M3 are the formation of ethylidene from vinyl (R*f*) and ethyl (R*j*), respectively (Figs. 2 and 3). In M2 on Pt(1 1 1), the rate-limiting step is the last one, the hydrogenation of vinylidene to ethylidyne (R*h*), whereas on Pd(1 1 1) the first step, ethylene dehydrogenation to vinyl (R*b*), determines the conversion rate (see above). Among all rate-limiting steps those of M2 are the fastest on both Pt(1 1 1) and Pd(1 1 1), suggesting that this mechanism should be the most plausible on either surface. There is also evidence from an analysis of possible reaction routes of vinyl and ethyl. The production of ethylidene species is unlikely in either case, thus excluding the reaction pathways M1 and M3. These previously unforeseen findings clearly highlight the value of the kMC simulations. Solely on the basis of the barriers obtained from our DFT calculations [27,29], we had concluded that ethylene dehydrogenation to vinyl (R*b*) should be the rate-limiting step during ethylene conversion to ethylidyne on Pd(1 1 1) [27] via M1 or M2, whereas on Pt(1 1 1) [29] one would expect two rate-limiting steps: ethylene dehydrogenation to vinyl (R*b*) and vinylidene hydrogenation to ethylidyne (R*h*). In contrast, kMC simulations take into account actual reaction conditions on the surface and in the gas phase. These simulations point to M2 as a clearly preferred conversion mechanism. Due to a deficit of surface hydrogen under the conditions assumed, hydrogenation steps are generally slower than the competing dehydrogenation steps, making M2 faster than M, which involves a very slow hydrogenation step, R*f*.

3.2.9. Apparent activation energies

Using the results of our simulations, we calculated the apparent activation energies of ethylidyne formation. As shown in Fig. 1S of Supplementary Data (SD), the rate of forming ethylidyne (the corresponding turnover frequency) increases with temperature. The apparent activation energies deduced from pertinent Arrhenius plots are 45 kJ mol^{-1} on Pt(1 1 1) and 94 kJ mol^{-1} on Pd(1 1 1), in agreement with experiments that showed the formation of ethylidyne formation to be easier on Pt(1 1 1) than on Pd(1 1 1) [58]. The theoretical apparent activation energy on Pd(1 1 1) agrees very well with the experimental value, 92 ± 4 kJ mol^{-1} [9]. The experimental values on Pt(1 1 1) are slightly higher than our kMC value. However, one should keep in mind that our kMC value is obtained from an Arrhenius plot in a notably larger range of temperatures, 250–400 K, while the experimental values were obtained from relatively narrow temperature ranges, e.g., 63 kJ mol^{-1} (250–280 K) [68], 67 kJ mol^{-1} (230–270 K) [69], 54–75 kJ mol^{-1} (230–250 K) [70]. If we restrict the analysis of our kMC results to the temperature range 250–330 K, the apparent activation energy for the formation of ethylidyne on Pt(1 1 1) becomes 65 kJ mol^{-1}, again in very good agreement with the experimental results.

3.3. Temperature dependence of surface coverages

Fig. 4 displays the surface coverages [34] θ of all detectable ($\theta > 0.01$) species on the surfaces Pd(1 1 1) and Pt(1 1 1) after 60 s of simulations as a function of the temperature. The maximum ethylidyne coverage achieved on both surfaces is 0.33 (Fig. 4), in good agreement with some experimental results on Pd(1 1 1) [14,71] while other experiments, on Pd(1 1 1) [12,72] and on Pt(1 1 1) [73], determined a saturation coverage of 0.25 only. The maximum coverage of ethylene achieved in our simulations on both surfaces is 0.25. Unfortunately, the saturation coverage of ethylene is problematic to determine accurately by experiment, due to lack of an ordered surface phase and the formation of multilayers [74]. Nevertheless, on Pd(1 1 1) ethylene coverage of 0.33 was obtained with indirect methods [10], while on Pt(1 1 1), a combination of nuclear reaction analysis and X-ray photoemission yielded ~0.25 coverage of ethylene on Pt(1 1 1), in agreement with our kMC result [73].

3.3.1. Evolution of coverages on Pd(1 1 1)

According to our simulations, the formation of ethylidyne on Pd(1 1 1) starts at ~330 K; however, the coverage remains low, 0.008, after 60 s of simulations (Fig. 4a). The ethylidyne coverage increases very fast, to 0.22, when the temperature increases from 330 K to 350 K; simultaneously the ethylene coverage decreases from 0.23 to 0.09. At temperatures above 375 K, the ethylidyne coverage is above 0.32, while the ethylene coverage drops below 0.01. The coverages of all intermediates are below 0.01, due to the fact that the first reaction step is the slowest one. Experiments on Pd(1 1 1) also did not detect any intermediates on the surface when ethylene is converted to ethylidyne [10,11,14,75]. Hydrogen coverage remains below 0.01 over the whole temperature range considered, due to the conversion of ethylene to ethane which irreversibly desorbs from the surface.

3.3.2. Evolution of coverages on Pt(1 1 1)

On Pt(1 1 1), we calculated significantly more species to accumulate on the surface during the transformation of ethylene (Fig. 4b). Recent studies on the conversion of di-σ ethylene at

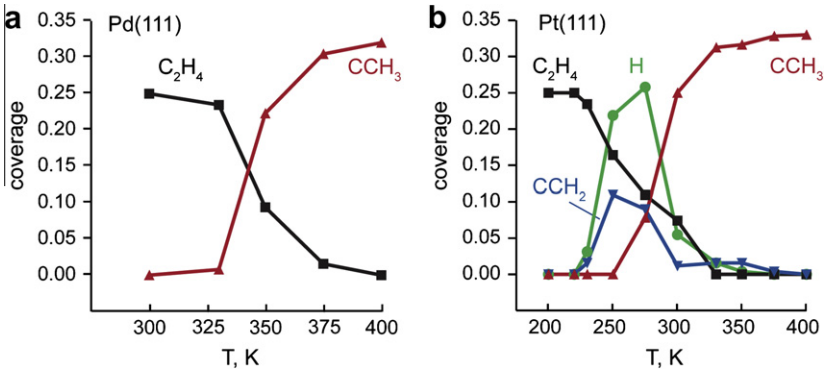

Fig. 4. Temperature dependence of the coverages θ of species detected on the surface ($\theta > 0.01$) after 60 s of simulation of ethylene conversion to ethylidyne on (a) Pd(1 1 1) and (b) Pt(1 1 1).

Pt(1 1 1) applying the sum frequency generation (SFG) spectroscopy [76] and reflection–absorption infrared spectroscopy (RAIRS) [77], observed a peak at 2957–2960 cm^{-1} and assigned it to the asymmetric stretch $\nu_a(CH_3)$ of the CH_3 group of ethylidene. In our recent DFT study [29], we calculated the vibrational frequencies of all intermediates and found that an IR frequency in that region is not specific for ethylidene, but could also be attributed to adsorbed vinyl or vinylidene.

In the present work, we calculated the conversion of ethylene on Pt(1 1 1) to start at temperatures as low as 230 K; ethylene coverage becomes essentially zero at temperatures above 325 K. However, the product at $T < 250$ K is not ethylidyne but vinylidene (Fig. 4b). In this context, recall the experimental observations of Zaera and Bernstein [15] who found on Pt(1 1 1) that vinyl requires the same temperature as ethylene to be converted to ethylidyne, ~300 K. This result was also confirmed by our simulations of vinyl species on Pt(1 1 1). These theoretical and experimental results can be rationalized by the fact that on Pt(1 1 1) the rate-limiting step for ethylene conversion to ethylidyne is the last one, the hydrogenation of vinylidene (R*h*). In contrast, on Pd(1 1 1), our simulations showed that conversion of vinyl to ethylidyne starts at a significantly lower temperature, 230 K, than the conversion of ethylene, 330 K, consistent with the *first* step of ethylene conversion (R*b*) being rate-controlling (see Section 3.1). On Pt(1 1 1), the coverage of vinylidene species starts to increase with increasing temperature and reaches a maximum at ~250 K, where it is ~0.11. Afterward, vinylidene starts to convert to ethylidyne and at $T > 300$ K, the coverage of vinylidene is already below 0.02. Ethylidyne appears on the surface at temperatures above 250 K and upon further heating ethylidyne starts to accumulate rapidly. Its coverage is already 0.25 at 300 K, and more than 0.30 at $T > 325$ K. As vinylidene and ethylidyne are products of dehydrogenation reactions, hydrogen is also present on Pt(1 1 1) at temperatures below 325 K. As already commented on, hydrogen leaves the Pt(1 1 1) surface mostly as H_2, rather than as C_2H_6. The surface coverage of H reaches its maximum $\theta_H \approx 0.26$ at $T = 275$ K for two reasons: (i) at temperatures 230–250 K, only dehydrogenation steps occur on the surface, i.e., ethylene converts to vinylidene (R*b* and R*g*) and (ii) the desorption of H (R*l*) has not started yet. Desorption starts at $T > 275$ K, and hence, the surface coverage of atomic H decreases rapidly so that *H* vanishes at $T > 330$ K. In their TPD experiments, Berlowitz et al. [65] also found a hydrogen desorption peak at 250 K in the spectra of ethylene adsorbed on Pt(1 1 1), while other experiments found it at a higher temperature, at ~300 K [1,16,78].

For specific temperatures, kMC simulations allow one to trace how the surface coverages of various species change as a function of time during the simulation; for details see Supplementary Data.

4. Conclusions

We carried out a first-principles-based kinetic Monte Carlo (kMC) study of how ethylene transforms into ethylidyne on the surfaces Pd(1 1 1) and Pt(1 1 1). At variance with earlier suggestions [15,24,32,76], we found that pathway M2, via vinyl and vinylidene should dominate on both surfaces. The other two mechanisms considered, M1 (via vinyl and ethylidene) and M3 (via ethyl and ethylidene), proceed via the rate-limiting formation of ethylidene from vinyl or ethyl, respectively. The rate-limiting steps in M1 and M3 are significantly slower than the rate-limiting step of M2; hence, M1 and M3 are ruled out by the present kMC simulations.

In agreement with experimental evidence, the kMC simulations predict the conversion of ethylene to ethylidyne occur at significantly lower temperatures on Pt(1 1 1) than on Pd(1 1 1). The calculated apparent activation energy of ethylidyne formation is also lower on Pt(1 1 1), 45 kJ mol^{-1}, than on Pd(1 1 1), 95 kJ mol^{-1}; both values are in good agreement with experimental results. As the rate-limiting step on Pt(1 1 1) is the last elementary step, namely, vinylidene hydrogenation to ethylidyne, vinylidene species can be accumulated on the surface, especially at temperatures below 300 K. In contrast, no intermediates were calculated to accumulate on Pd(1 1 1) because the first reaction step is rate-limiting (together with the third one). We also determined that hydrogen, produced during ethylene conversion to ethylidyne, leaves the Pt(1 1 1) surface predominantly as H_2, but is removed from Pd(1 1 1) through the hydrogenation of ethylene to ethane.

In general, our kMC simulations demonstrated that even in a relatively simple reaction network, as the one discussed in the present study, the determination of the fastest route of the overall process and of the associated rate-limiting steps cannot be unequivocally predicted if based only on activation energies. The reaction rates depend on the initial conditions, of course, e.g., in the present case on the concentration of H atoms on the surface. In the simulations discussed, the hydrogenation steps were found to be slow due to the limited production of adsorbed hydrogen atoms. This leads to the somewhat counterintuitive result that in several cases hydrogenation steps with lower barriers are slower than dehydrogenation steps with higher barriers.

Acknowledgments

H.A.A. thanks the Bulgarian National Science Fund (National Center of Advanced Materials UNION) for support. This work was supported by a Laboratory Directed Research and Development (LDRD) project at the Pacific Northwest National Laboratory (PNNL). N.R. acknowledges financial support by Deutsche Forschungsgemeinschaft and Fonds der Chemischen Industrie (Germany).

Appendix A. Supplementary material

Supplementary data associated with this article can be found, in the online version, at doi:10.1016/j.jcat.2011.09.035.

References

[1] H. Steininger, H. Ibach, S. Lehwald, Surf. Sci. 117 (1982) 685.
[2] A. Cassuto, M. Mane, J. Jupille, Surf. Sci. 249 (1991) 8.
[3] A. Cassuto, J. Kiss, J.M. White, Surf. Sci. 255 (1991) 289.
[4] J. Stöhr, F. Sette, A.L. Johnson, Phys. Rev. Lett. 53 (1984) 1684.
[5] R.J. Koestner, J. Stöhr, J.L. Gland, J.A. Horsley, Chem. Phys. Lett. 105 (1984) 332.
[6] P.S. Cremer, G.A. Somorjai, J. Chem. Soc. Faraday Trans. 91 (1995) 3671.
[7] M.B. Hugenschmidt, P. Dolle, J. Jupille, A. Cassuto, J. Vac. Sci. Technol. A. 7 (1989) 3312.
[8] J. Kubota, S. Ichihara, J.N. Kondo, K. Domen, C. Hirose, Surf. Sci. 357–358 (1996) 634.
[9] D. Stacchiola, F. Calaza, T. Zheng, W.T. Tysoe, J. Mol. Catal. A 228 (2005) 35.
[10] W.T. Tysoe, G.L. Nyberg, R.M. Lambert, J. Phys. Chem. 88 (1984) 1960.
[11] L.L. Kesmodel, J.A. Gates, Surf. Sci. 111 (1981) L747.
[12] D. Stacchiola, M. Kaltchev, G. Wu, W.T. Tysoe, Surf. Sci. 470 (2000) L32.
[13] T.P. Beebe Jr., J.T. Yates, J. Am. Chem. Soc. 108 (1986) 663.
[14] M. Sock, A. Eichler, S. Surnev, J.N. Andersen, B. Klötzer, K. Hayek, M.G. Ramsey, F.P. Netzer, Surf. Sci. 545 (2003) 122.
[15] F. Zaera, N. Bernstein, J. Am. Chem. Soc. 116 (1994) 4881.
[16] F. Zaera, Langmuir 12 (1996) 88.
[17] R.J. Koestner, M.A. van Hove, G.A. Somorjai, Surf. Sci. 121 (1982) 321.
[18] Ts.S. Marinova, K.L. Kostov, Surf. Sci. 181 (1987) 573.
[19] M.M. Hills, J.E. Parmeter, C.B. Mullins, W.H. Weinberg, J. Am. Chem. Soc. 108 (1986) 3554.
[20] H. Gabasch, K. Hayek, B. Klötzer, A. Knop-Gericke, R. Schlögl, J. Phys. Chem. B 110 (2006) 4947.
[21] I. Jungwirthová, L.L. Kesmodel, J. Phys. Chem. B 105 (2001) 674.
[22] R. Deng, E. Herceg, M. Trenary, Surf. Sci. 573 (2004) 310.
[23] R. Deng, E. Herceg, M. Trenary, J. Am. Chem. Soc. 127 (2005) 17628.
[24] M. Neurock, R.A. van Santen, J. Phys. Chem. B 104 (2000) 11127.
[25] V. Pallassana, M. Neurock, V.S. Lusvardi, J.J. Lerou, D.D. Kragten, R.A. van Santen, J. Phys. Chem. B 106 (2002) 1656.
[26] L.V. Moskaleva, Z.-X. Chen, H.A. Aleksandrov, A.B. Mohammed, Q. Sun, N. Rösch, J. Phys. Chem. C 113 (2009) 2512.

[27] L.V. Moskaleva, H.A. Aleksandrov, D. Basaran, Z.-J. Zhao, N. Rösch, J. Phys. Chem. C 113 (2009) 15373.
[28] J. Andersin, N. Lopez, K. Honkala, J. Phys. Chem. C 113 (2009) 8278.
[29] Z.-J. Zhao, L.V. Moskaleva, H.A. Aleksandrov, D. Basaran, N. Rösch, J. Phys. Chem. C 114 (2010) 12190.
[30] Y. Chen, D.G. Vlachos, J. Phys. Chem. C 114 (2010) 4973.
[31] M. Li, W. Guo, R. Jiang, L. Zhao, X. Lu, H. Zhu, D. Fu, H. Shan, J. Phys. Chem. C 114 (2010) 8440.
[32] F. Zaera, C.R. French, J. Am. Chem. Soc. 121 (1999) 2236.
[33] A.T. Anghel, D.J. Wales, S.J. Jenkins, D.A. King, J. Chem. Phys. 126 (2007) 044710.
[34] We define the surface coverage θ as the fraction of the adsorption sites that are occupied. θ = 1 (ML) refers to the metal atom density on the (1 1 1) surface. We will thus refrain from using the qualifier "monolayer" or ML.
[35] D. Stacchiola, S. Azad, L. Burkholder, W.T. Tysoe, J. Phys. Chem. B 105 (2001) 11233.
[36] F. Zaera, Surf. Sci. 219 (1989) 453.
[37] M.E. Pansoy-Hjelvik, R. Xu, Q. Gao, K. Weller, F. Feher, J.C. Hemminger, Surf. Sci. 312 (1994) 97.
[38] V.P. Zhdanov, Elementary Physicochemical Processes on Solid Surfaces, Plenum Press, New York, 1991.
[39] K. Reuter, in: O. Deutschmann (Ed.), Modeling Heterogeneous Catalytic Reactions: From the Molecular Process to the Technical System, Wiley VCH, Weinberg, 2009.
[40] K. Reuter, M. Scheffler, Phys. Rev. B 73 (2006) 045433.
[41] C. Sendner, S. Sakong, A. Groβ, Surf. Sci. 600 (2006) 3258.
[42] D.H. Mei, M. Neurock, C.M. Smith, J. Catal. 268 (2009) 181.
[43] D.H. Mei, J.C. Du, M. Neurock, Ind. Eng. Chem. Res. 49 (2010) 10364.
[44] E.W. Hansen, M. Neurock, Chem. Eng. Sci. 54 (1999) 3411.
[45] E.W. Hansen, M. Neurock, J. Catal. 196 (2000) 241.
[46] E.W. Hansen, M. Neurock, J. Phys. Chem. B 105 (2001) 9218.
[47] M. Neurock, D.H. Mei, Top. Catal. 20 (2002) 5.
[48] D.H. Mei, E.W. Hansen, M. Neurock, J. Phys. Chem. B 107 (2003) 798.
[49] L.D. Kieken, M. Neurock, D.H. Mei, J. Phys. Chem. B 109 (2005) 2234.
[50] D.H. Mei, P.A. Sheth, M. Neurock, C.M. Smith, J. Catal. 242 (2006) 1.
[51] G. Kresse, J. Hafner, Phys. Rev. B 49 (1994) 14251.
[52] G. Kresse, J. Furthmüller, Comput. Mater. Sci. 6 (1996) 15.
[53] J.P. Perdew, Y. Wang, Phys. Rev. B 45 (1992) 13244.
[54] Z.-X. Chen, H.A. Aleksandrov, D. Basaran, N. Rösch, J. Phys. Chem. C 114 (2010) 17683.
[55] H. Molero, B.F. Bartlett, W.T. Tysoe, J. Catal. 181 (1999) 49. and references therein.
[56] L. Burkholder, D. Stacchiola, W.T. Tysoe, Surf. Rev. Lett. 10 (2003) 909.
[57] Recall the IUPAC definition of a rate-determining (rate-limiting or rate-controlling) step: an elementary reaction the rate constant for which exerts a strong effect–stronger than that of any other rate constant – on the overall rate, <http://goldbook.iupac.org>.
[58] L.P. Wang, W.T. Tysoe, R.M. Ormerod, R.M. Lambert, H. Hoffmann, F. Zaera, J. Phys. Chem. 94 (1990) 4236.
[59] M.K. Ko, H. Frei, J. Phys. Chem. B 108 (2004) 1805.
[60] W. Wasylenko, H. Frei, J. Phys. Chem. B 109 (2005) 16873.
[61] M. Salmeron, G.A. Somorjai, J. Phys. Chem. 86 (1982) 341.
[62] J.M. Essen, J. Haubrich, C. Becker, K. Wandelt, Surf. Sci. 601 (2007) 3472.
[63] R.G. Windham, M.E. Bartram, B.E. Koel, J. Phys. Chem. 92 (1988) 2862.
[64] B. Hammer, L.B. Hansen, J.K. Nørskov, Phys. Rev. B 59 (1999) 7413.
[65] P. Berlowitz, C. Megiris, J.B. Butt, H.H. Kung, Langmuir 1 (1985) 206.
[66] We carried out simulations starting with adsorbed vinyl species, θ(vinyl) = 0.20, on both Pt(1 1 1) and Pd(1 1 1) at a number of temperatures, starting from 100 K.
[67] S. Azad, M. Kaltchev, D. Stacchiola, G. Wu, W.T. Tysoe, J. Phys. Chem. B 104 (2000) 3107.
[68] F. Zaera, J. Am. Chem. Soc. 111 (1989) 4240.
[69] W. Erley, Y. Li, D.P. Land, J.C. Hemminger, Surf. Sci. 103 (1994) 177.
[70] S.B. Mohsin, M. Trenary, H. Robota, J. Chem. Phys. Lett. 154 (1989) 511.
[71] J.A. Gates, L.L. Kesmodel, Surf. Sci. Lett. 120 (1982) L461.
[72] D. Stacchiola, W.T. Tysoe, J. Phys. Chem. C 113 (2009) 8000.
[73] K. Griffiths, W.N. Lennard, I.V. Mitchell, P.R. Norton, G. Pirug, H.P. Bonzel, Surf. Sci. Lett. 284 (1993) L389.
[74] D. Stacchiola, L. Burkholder, W.T. Tysoe, Surf. Sci. 511 (2002) 215.
[75] M. Kaltchev, A.W. Thompson, W.T. Tysoe, Surf. Sci. 391 (1997) 145.
[76] P. Cremer, C. Stanners, J.W. Niemantsverdriet, Y.R. Shen, G. Somorjai, Surf. Sci. 328 (1995) 111.
[77] R. Deng, E. Herceg, M. Trenary, Surf. Sci. 560 (2004) L195.
[78] M. Yata, R.J. Madix, Surf. Sci. 328 (1995) 171.